Published in final edited form as:
Cell. 2012 October 26; 151(3): 645–657. doi:10.1016/j.cell.2012.09.020.

GABAergic RIP-Cre Neurons in the Arcuate Nucleus Selectively Regulate Energy Expenditure

Dong Kong[1,6], **Qingchun Tong**[1,2,6], **Chianping Ye**[1], **Shuichi Koda**[1,3], **Patrick M. Fuller**[4], **Michael J. Krashes**[1], **Linh Vong**[1], **Russell S. Ray**[5], **David P. Olson**[1], and **Bradford B. Lowell**[1,*]

[1]Division of Endocrinology, Department of Medicine, Beth Israel Deaconess Medical Center and Harvard Medical School, Boston, MA 02115, USA

[2]Brown Foundation Institute of Molecular Medicine, University of Texas Health Science Center at Houston, Houston, TX 77030, USA

[3]Asubio Pharma Co., Ltd. Kobe 650-0047, Japan

[4]Department of Neurology, Beth Israel Deaconess Medical Center and Harvard Medical School, Boston, MA 02115, USA

[5]Department of Genetics, Harvard Medical School, Boston, MA 02115, USA

INTRODUCTION

Neural circuits operating within and extending beyond the hypothalamus regulate food intake and energy expenditure. Proopiomelanocortin (POMC)-expressing neurons and adjacent agouti-related peptide (AgRP)-expressing neurons, both located in the arcuate nucleus (ARC) of the hypothalamus, are key components of this circuitry. The ARC also contains many other neurons that express neither POMC nor AgRP (i.e. non-POMC, non-AgRP neurons). Due to their location in the ARC, these could also regulate energy balance. A subset of these “non-POMC, non-AgRP” neurons have clear neuroendocrine functions, such as those expressing kisspeptin, growth hormone-releasing hormone or dopamine. “Non-POMC, non-AgRP” neurons whose function is something other than neuroendocrine also likely exist. These neurons, like POMC and AgRP neurons, could be additional, important regulators of energy balance.

In *Rip-Cre* transgenic mice (Postic et al., 1999), the rat insulin-2 (*Ins2*) promoter drives cre expression in both pancreatic β-cells and the brain (Song et al., 2010; Wicksteed et al., 2010). Neurons expressing cre activity, hereafter referred to as “RIP-Cre neurons”, are distributed in many hypothalamic sites, including the ARC. Within the ARC, RIP-Cre neurons are intermingled with, but are distinct from, POMC and AgRP neurons (Choudhury et al., 2005). Deletion of various loxed alleles in *Rip-Cre* mice, often with the initial intent of manipulating gene expression in pancreatic β cells, has marked effects on energy balance (Chakravarthy et al., 2007; Choudhury et al., 2005; Covey et al., 2006; Kubota et al., 2004;

*Correspondence: blowell@bidmc.harvard.edu.
[6]These authors contribute equally to this work

SUPPLEMENTAL INFORMATION
Supplemental Information includes Extended Experimental Procedures, seven figures, and two tables and can be found online …

Lin et al., 2004; Mori et al., 2009). It is generally believed that this is secondary to altered function of RIP-Cre neurons as opposed to pancreatic β cells. Notably, disruption of leptin signaling in *Rip-Cre* transgenic mice causes obesity (Covey et al., 2006). As RIP-Cre neurons are found in many locations in the brain, the specific subgroup of RIP-Cre neurons responsible for regulating energy balance is unknown. Similarly, the relevant neurotransmitter(s) and downstream circuitry are likewise unknown.

Synaptic transmission via glutamate and GABA are critical components of the hypothalamic circuitry regulating energy balance (Cowley et al., 2001; Liu et al., 2012; Pinto et al., 2004; Tong et al., 2008; van den Pol, 2003; Vong et al., 2011; Wu et al., 2009; Yang et al., 2011). Consequently, it is of interest to establish if synaptic release of glutamate or GABA, specifically by RIP-Cre neurons, regulates energy balance. For the purpose of addressing such questions, we previously generated mice with loxed alleles of the vesicular glutamate transporter 2 (VGLUT2, required for synaptic release of glutamate from hypothalamic neurons) and the vesicular GABA transporter (VGAT, required for synaptic release of GABA from all GABAergic neurons) (Tong et al., 2007; Tong et al., 2008). In the present study, we have deleted *Vglut2* and *Vgat* specifically from RIP-Cre neurons. This has uncovered a critical role for synaptic release of GABA, but not glutamate, from RIP-Cre neurons, in selectively stimulating energy expenditure. Using pharmacogenetic techniques (Alexander et al., 2009; Krashes et al., 2011), we go on to establish that RIP-Cre neurons located specifically in the ARC drive this effect. Finally, using channelrhodopsin-assisted circuit mapping (Atasoy et al., 2008; Petreanu et al., 2007), we identify the downstream circuitry selectively engaged by ARC RIP-Cre neurons.

RESULTS

Neuronal Expression of Cre Recombinase in *Rip-Cre* Transgenic Mice

Rip-Cre transgenic mice were crossed with cre-dependent green fluorescent protein (GFP) reporter mice (Novak et al., 2000) to generate *Rip-Cre, lox-GFP* mice and immunohistochemistry for GFP was performed. GFP-positive neurons (i.e. RIP-Cre neurons) were primarily found in the hypothalamus and occasionally in the cortex and striatum (Figure 1A and Table S1). Within the hypothalamus, GFP-positive neurons were observed in the arcuate nucleus (ARC), the ventromedial hypothalamus (VMH), the medial tuberal nucleus (MTu), the suprachiasmatic nucleus (SCN), and the dorsomedial hypothalamus (DMH). These observations are consistent with previous reports (Choudhury et al., 2005; Lin et al., 2004; Song et al., 2010; Wicksteed et al., 2010).

Generation of Mice Lacking VGAT in RIP-Cre Neurons

Rip-Cre transgenic mice were crossed with $Vgat^{flox/flox}$ mice. The resulting *Rip-Cre,* $Vgat^{flox/+}$ mice were then crossed with $Vgat^{flox/flox}$ mice to obtain *Rip-Cre,* $Vgat^{flox/flox}$ study subjects and their control littermates ($Vgat^{flox/flox}$ mice and *Rip-Cre*, $Vgat^{flox/+}$ mice). *Rip-Cre*, $Vgat^{flox/+}$ littermates were included as controls to rule out nonspecific effects of the *Rip-Cre* transgene (Lee et al., 2006). *In situ* hybridization studies for *Vgat* mRNA were then performed to assess for GABAergic neurons and also for sites where the *Rip-Cre* transgene disrupts *Vgat* expression. In $Vgat^{flox/flox}$ control mice, *Vgat* mRNA signal was detected in sites known to contain GABAergic neurons. With regards to sites shown in Figure 1B, these include, within the hypothalamus - the ARC, DMH and MTu; and beyond the hypothalamus - the central amygdala (CeA) and the reticular nucleus of thalamus (RT). In *Rip-Cre*, $Vgat^{flox/flox}$ mice (Figure 1C), *Vgat* signal was substantially reduced in sites containing RIP-Cre neurons, such as the ARC, DMH, and MTu. In sites where RIP-Cre neurons are not found, such as the CeA and RT, *Vgat* signal, as expected, was unchanged. Finally, we measured *Vgat* mRNA levels in the mediobasal hypothalamus, a region that

includes the ARC, DMH, and MTu, which are three sites suggested by the above analysis to contain GABAergic RIP-Cre neurons. This quantitative analysis confirmed that *Vgat* mRNA, but not that of a control transcript (*Ucp2* mRNA), was substantially reduced in *Rip-Cre*, $Vgat^{flox/flox}$ mice (Figure 1D).

Vgat mRNA was undetectable in both control and *Rip-Cre*, $Vgat^{flox/flox}$ pancreatic islets (Figure 1E), while, as noted above, using the identical assay, *Vgat* mRNA was readily detected in the hypothalamus (Figure 1D). Confirming the intact nature of pancreatic islet RNA, *Ucp2*, a gene expressed in islets (Zhang et al., 2001), was readily detected in the same samples (Figure 1E). Thus, mouse islets express little or no *Vgat* mRNA. Consequently, deletion of the *Vgat* gene in pancreatic β cells should produce no effects.

Energy Balance in Mice Lacking VGAT in RIP-Cre Neurons

When fed a standard chow diet, *Rip-Cre*, $Vgat^{flox/flox}$ mice have modestly increased body weight (Figure 2A) and, at 3 months of age, markedly increased fat stores (Figure 2B). Lean body mass, on the other hand, was unchanged (data not shown). The possible causes of positive energy balance were then assessed in 2-month-old animals. Food intake (Figure 2C) and locomotor activity (Figure 2D) were found to be unchanged. Obesity, in the face of normal food intake, strongly implicates reduced energy expenditure in *Rip-Cre*, $Vgat^{flox/flox}$ mice. This was confirmed by direct assessments of energy expenditure. Oxygen consumption was markedly reduced in *Rip-Cre*, $Vgat^{flox/flox}$ mice and this was apparent when data was expressed per body weight (Figure 2E) or per animal (Figure 2F). Thus, obesity in *Rip-Cre*, $Vgat^{flox/flox}$ mice is due entirely to a selective reduction in energy expenditure.

We next analyzed brown adipose tissue (BAT), a well-established mediator of thermogenesis (Cannon and Nedergaard, 2004). Interscapular BAT (iBAT) of *Rip-Cre*, $Vgat^{flox/flox}$ mice was markedly enlarged and pale in comparison with that from control littermates. As shown in Figure 2G, BAT from *Rip-Cre*, $Vgat^{flox/flox}$ mice contained larger cells with unilocular triglyceride deposits, similar to that observed in animals with defective sympathetic activation of BAT (Bachman et al., 2002). As assessed by biotelemetry probes implanted subcutaneously in the interscapula fossa beneath iBAT (Enriori et al., 2011), iBAT temperature, an index of BAT thermogenesis, was reduced in *Rip-Cre*, $Vgat^{flox/flox}$ mice (Figure 2H). In contrast, subcutaneous temperature of a flank site devoid of BAT was similar in the two groups (Figure S1A). Finally, expression of *Ucp1* mRNA, which encodes the BAT-specific thermogenic molecule, uncoupling protein 1, was significantly lower in *Rip-Cre*, $Vgat^{flox/flox}$ mice (Figure 2I). These results indicate that GABA release from RIP-Cre neurons regulates BAT thermogenic function and suggest that decreased BAT activity is, at least in part, responsible for reduced energy expenditure in *Rip-Cre*, $Vgat^{flox/flox}$ mice.

Given that *Rip-Cre* transgenic mice express cre in some SCN neurons (Figure S1B) and that virtually all SCN neurons are GABAergic (Figure S1C), *Rip-Cre*, $Vgat^{flox/flox}$ mice could have altered circadian regulation, which could in turn affect energy balance (Bass and Takahashi, 2010). To address this possibility, body temperature (Tb), a reliable indicator of circadian clock activity (Fuller et al., 2008), was measured using implanted biotelemetry. As shown in Figure S1D,E, *Rip-Cre*, $Vgat^{flox/flox}$ mice displayed diurnal and circadian Tb patterns (phasing, amplitude, or period) that were comparable to controls. Thus, the circadian clock does not appear to be altered or otherwise dysfunctional in *Rip-Cre*, $Vgat^{flox/flox}$ mice and unlikely contributes to the metabolic phenotypes of the *Rip-Cre*, $Vgat^{flox/flox}$ mice. Likewise, serum T4 and corticosterone levels, two other potential regulators of energy balance, were found to be unchanged in *Rip-Cre*, $Vgat^{flox/flox}$ mice (Figure S1F,G).

Energy Balance in Mice Lacking VGLUT2 in RIP-Cre Neurons

Some RIP-Cre neurons are glutamatergic, such as those in the VMH. To assess if glutamatergic RIP-Cre neurons regulate energy homeostasis, mice lacking VGLUT2 in RIP-Cre neurons (*Rip-Cre, Vglut2*$^{flox/flox}$ mice) were generated as was done for *Rip-Cre, Vgat*$^{flox/flox}$ mice. *In situ* hybridization analyses revealed that, as expected, *Vglut2* mRNA was dramatically reduced in the VMH of *Rip-Cre, Vglut2*$^{flox/flox}$ mice (Figure S2A,B). Of note, *Rip-Cre, Vglut2*$^{flox/flox}$ mice had normal body weight, oxygen consumption, and food intake (Figure S2C–E), indicating that glutamate release from RIP-Cre neurons is not required for regulation of energy balance.

Diet-induced Obesity in Mice Lacking VGAT in RIP-Cre Neurons

Increased energy expenditure following the ingestion of highly palatable, calorically dense diets, a phenomenon often referred to as diet-induced thermogenesis, plays an important role in resisting diet-induced obesity (Bachman et al., 2002). To determine if GABAergic RIP-Cre neuron-driven energy expenditure is involved in this adaptive response, *Rip-Cre, Vgat*$^{flox/flox}$ mice and control animals were fed a high-fat, high-sucrose diet (HFD) from between 6 to 26 weeks of age. As shown in Figure 3A, compared to control mice, *Rip-Cre, Vgat*$^{flox/flox}$ mice developed massive obesity. Of interest, this diet-induced obesity was not caused by increased food intake (Figure 3B), strongly implicating impaired diet-induced thermogenesis. To directly assess this, oxygen consumption was measured during the transition from chow to HFD (3 days on chow followed by 3 days on HFD) in 7 week old mice (note, body weight is normal at this early age). As shown in Figure 3C, oxygen consumption of *Rip-Cre*, *Vgat*$^{flox/flox}$ mice, on both chow and HFD, was markedly lower than that observed in control animals. Importantly, while HFD increased energy expenditure by 7–12% in control mice, this response was markedly blunted in *Rip-Cre*, *Vgat*$^{flox/flox}$ mice (increased by only 3–5% in response to HFD). In addition, HFD-treated *Rip-Cre*, *Vgat*$^{flox/flox}$ mice (6-month old and 20 weeks on HFD) exhibited reduced *Ucp1* mRNA expression in BAT (Figure 3D). In summary, *Rip-Cre*, *Vgat*$^{flox/flox}$ mice are extremely sensitive to diet-induced obesity, and this is due entirely to a defect in diet-induced thermogenesis.

Effects of Leptin Treatment in Mice Lacking VGAT in RIP-Cre Neurons

Genetic deletion of leptin receptors (LEPRs) from RIP-Cre neurons causes marked obesity without affecting food intake (Covey et al., 2006), suggesting a defect in energy expenditure. Given that *Rip-Cre*, *Vgat*$^{flox/flox}$ mice also have defective energy expenditure, this raises the possibility that GABA release from RIP-Cre neurons mediates leptin's effects on energy expenditure. To test this, changes in body weight and food intake were monitored following injection of saline or leptin. In control mice, treatment with leptin reduced body weight (Figure 4A,B) and food intake (Figure 4C,D). Of note, while the ability of leptin to reduce food intake in *Rip-Cre, Vgat*$^{flox/flox}$ mice was completely intact (Figure 4D), its ability to reduce body weight was markedly attenuated (Figure 4B). Attenuation of body weight loss in the face of intact inhibition of food intake indicates that leptin's ability to increase energy expenditure is impaired in *Rip-Cre, Vgat*$^{flox/flox}$ mice. To directly assess leptin action on energy expenditure, in particular, in stimulating BAT activity, iBAT temperature and *Ucp1* mRNA were measured. In control mice, leptin but not saline dramatically and rapidly increased the temperature of iBAT (as previously described (Enriori et al., 2011)) (Figure 4E,F), but not the temperature of a subcutaneous flank site devoid of BAT (Figure S3A,B). Leptin also markedly increased *Ucp1* mRNA levels (Figure 4G). Of note, these stimulatory effects of leptin on iBAT temperature and *Ucp1* mRNA levels were attenuated in *Rip-Cre, Vgat*$^{flox/flox}$ animals (Figure 4E–G). Thus, GABA release from RIP-Cre neurons is required for leptin to fully stimulate energy expenditure, but not for leptin to inhibit feeding.

To determine which subset of RIP-Cre neurons in the hypothalamus expresses leptin receptors (LEPRs), leptin-induced phosphorylation of STAT3 (Tyr705, pSTAT3), a marker for LEPR activity (Munzberg et al., 2004), was assessed in *Rip-Cre, lox-GFP* mice. The neurons double positive for pSTAT3 and RIP-Cre activity were mainly observed in the ARC and the VMH (Figure 4H,I and Figure S3C–N). The DMH, which contained both RIP-Cre neurons and pSTAT3-positive neurons, exhibited negligible co-localization (Figure 4I and Figure S3I–K). Since VMH neurons are glutamatergic and not GABAergic (Vong et al., 2011), all leptin-responsive, GABAergic RIP-Cre neurons appear to be located in the ARC. Collectively, given the above observations, it is likely that GABAergic RIP-Cre neurons in the ARC mediate leptin's stimulatory effect on energy expenditure.

Pharmacogenetic Activation of RIP-Cre Neurons in the ARC

To directly test the ability of ARC RIP-Cre neurons to drive energy expenditure, we used the pharmacogenetic approach referred to designer receptors exclusively activated by designer drugs (DREADD). The stimulatory DREADD, hM3Dq, is activated by the otherwise inert, brain penetrable compound, clozapine-N-oxide (CNO) (Alexander et al., 2009). The cre-dependent adeno-associated virus, AAV-Flex-hM3Dq-mCherry (Krashes et al., 2011), was stereotaxically injected into the ARC of 3–4 weeks old *Rip-Cre* transgenic mice (Figure 5A) and studies were performed 2–3 weeks after injection. Brain slice electrophysiology studies confirmed that CNO depolarizes and increases the firing rate of hM3Dq-expressing RIP-Cre neurons (Figure 5B), but not control non-hM3Dq-expressing RIP-Cre neurons (Figure S4A). hM3Dq virus was then bilaterally injected into the ARC of 5–6 week-old $Vgat^{flox/flox}$ mice, *Rip-Cre* mice, or *Rip-Cre*, $Vgat^{flox/flox}$ mice. Studies were performed 3 weeks after injection. The mCherry fusion tag was exclusively detected in the ARC of *Rip-Cre* mice and *Rip-Cre*, $Vgat^{flox/flox}$ mice, and was absent in the ARC of $Vgat^{flox/flox}$ mice (as these mice lack cre activity which enables hM3Dq expression) (Figure 5C). When CNO was injected *in vivo*, c-fos immunoreactivity was markedly increased in the ARC of *Rip-Cre* mice and *Rip-Cre*, $Vgat^{flox/flox}$ mice, but not in the ARC of $Vgat^{flox/flox}$ mice (Figure 5D). Thus, *in vivo* treatment with CNO activates hM3Dq-expressing RIP-Cre neurons in the ARC.

To assess effects on energy expenditure, virus-injected animals were housed individually in metabolic cages and oxygen consumption was monitored following injection with saline or CNO. After an acclimation period, each mouse was injected with saline on the first day followed by CNO on the second day. Selective activation of ARC RIP-Cre neurons with CNO rapidly increased oxygen consumption (Figure 5F) and this effect lasted for approximately 9 hours. Importantly, CNO had no effect on oxygen consumption in *Rip-Cre*, $Vgat^{flox/flox}$ mice (Figure 5G), which are notable for their inability to release GABA. Similarly, CNO had no effect on oxygen consumption in control mice (i.e. $Vgat^{flox/flox}$ mice), which do not express hM3Dq (Figure 5E). Remarkably, and consistent with our earlier findings suggesting that GABAergic RIP-Cre neurons selectively control energy expenditure, food intake was unaltered by CNO treatment (Figure S4B). We next assessed BAT activity during stimulation of ARC RIP-Cre neurons. In *Rip-Cre* mice, CNO significantly increased iBAT temperature (Figure 5I), but not subcutaneous flank temperature (Figure S4C), and also markedly increased *Ucp1* mRNA (Figure 5L). CNO did not stimulate iBAT temperature or *Ucp1* mRNA in $Vgat^{flox/flox}$ mice (which do not express hM3Dq) or in *Rip-Cre*, $Vgat^{flox/flox}$ mice (which are unable to release GABA) (Figures 5H,J,K,M). These results demonstrate that synaptic GABA release from ARC RIP-Cre neurons selectively stimulates BAT activity and energy expenditure.

Electrophysiologic Effects of Leptin on ARC RIP-Cre Neurons

Whole-cell current-clamp recordings were performed as previously described (Dhillon et al., 2006) on arcuate RIP-Cre neurons visualized by expression of GFP in *Rip-Cre, lox-GFP* mice. In data not shown, ARC RIP-Cre neurons exhibited heterogeneous responses to leptin: 30% of neurons (6/20) were excited (depolarized membrane potential and increased firing rate), 35% (7/20) were inhibited (hyperpolarized membrane potential and decreased firing rate), and 35% (7/20) were not affected by leptin. As discussed in the following section, the paraventricular hypothalamus (PVH) is the likely downstream site that mediates the thermogenic effects of GABAergic ARC RIP-Cre neurons. To assess the effects of leptin on PVH-projecting ARC RIP-Cre neurons, retrograde red fluorescent beads were stereotaxically injected into the PVH of *Rip-Cre, lox-GFP* mice (Figure S5A–B). Retrogradely transported beads were observed in sites known to innervate the PVH, including the ARC, DMH, SCN, nucleus of the solitary tract (NTS), and posterodorsal amygdala (MEpd) (data not shown). In the ARC, 62% (194 of 312) of RIP-Cre neurons contained red beads (Figure S5C). Recordings were then performed on PVH-projecting (GFP^+/$beads^+$) and in non-PVH-projecting (GFP^+/$beads^-$) ARC RIP-Cre neurons. Ionotropic glutamate (kynurenate) and GABA (PTX) receptor blockers were added to minimize indirect effects of leptin. As shown in Figure S5D, 9 of 15 PVH-projecting ARC RIP-Cre neurons were directly excited by leptin, 6 of 15 were unaffected by leptin and 0 of 15 were inhibited by leptin. In contrast, 0 of 12 non-PVH-projecting ARC RIP-Cre neurons were excited by leptin, 9 of 12 were unaffected by leptin, and 3 of 12 were directly inhibited by leptin (Figure S5E). Thus, leptin excites the majority of PVH-projecting ARC RIP-Cre neurons.

Downstream Neurocircuitry Engaged by ARC RIP-Cre Neurons

We next used channelrhodopsin2 (ChR2)-assisted circuit mapping (Atasoy et al., 2008; Petreanu et al., 2007) to identify proximal downstream neurons that could mediate stimulation of energy expenditure by GABAergic ARC RIP-Cre neurons. A virus that conditionally expresses ChR2-mCherry fusion protein (AAV-Flex-ChR2(H134R)-mCherry) (Zhang et al., 2007) in the presence of cre recombinase was unilaterally injected into the ARC of 3–4 week-old *Rip-Cre* mice (Figure 6A). Mice were studied 2–3 weeks after injection. Expressed ChR2 was functional as evidenced by light-evoked action potentials in RIP-Cre neurons (Figure 6B and Figure S6A–C). mCherry-positive dendrites and soma were abundantly and exclusively detected in the ARC (Figure 6C,D). mCherry-expressing axons were primarily observed in the PVH (Figure 6E). By comparison, much less abundant, scattered mCherry-expressing axons were seen in the DMH, the bed nuclei of the stria terminalis (BST), and the medial preoptic area (MPO) (Figure 6E and Table S2). Thus, the PVH is the dominant target of ARC RIP-Cre neurons. This is of interest because it has been suggested that release of GABA in the PVH stimulates brown adipose tissue thermogenesis (Madden and Morrison, 2009). To determine if GABAergic RIP-Cre neurons are functionally, synaptically connected to PVH neurons, inhibitory postsynaptic currents (IPSCs) were assessed in PVH neurons following illumination of ChR2-expressing RIP-Cre terminals. Light-driven IPSCs were reliably evoked in a small subset of randomly selected PVH neurons that were surrounded by mCherry fluorescent terminals (2 out of 14), and these were completely blocked by bicuculine, a $GABA_A$ receptor antagonist (Figure 6F). The latency between onset of light and onset of IPSC in these two neurons was 1.2 and 2.3 msec. The low frequency of responders (i.e. 2 out of 14) likely relates to complexity within the PVH, which is composed of numerous subsets of functionally distinct neurons (Biag et al., 2012; Simmons and Swanson, 2009). As explained below, we have used site of projection to enrich for PVH neurons likely to control energy expenditure, and therefore likely to receive monosynaptic input from GABAergic RIP-Cre neurons.

Given that the NTS receives abundant projections from the PVH (Geerling et al., 2010), contains neurons in polysynaptic contact with BAT (Bamshad et al., 1999; Cano et al., 2003; Oldfield et al., 2002), is known to regulate sympathetic outflow (Spyer, 1994) and inhibit BAT function (Cao et al., 2010), we hypothesized that PVH neurons projecting to the NTS drive RIP-Cre neuron-mediated energy expenditure. To test if NTS-projecting PVH neurons receive monosynaptic input from GABAergic ARC RIP-Cre neurons, dual injection studies were performed as illustrated in Figure 7A, with AAV-Flex-ChR2(H134R)-mCherry virus injected into the ARC and retrograde green fluorescent beads injected into the NTS of *Rip-Cre* mice. Histologic studies confirmed injection of beads into the NTS and, unavoidably, the nearby dorsal motor nucleus of the vagus nerve (DMV) (Figure S7A). Correct targeting of the NTS is further confirmed by the presence of retrogradely transported beads in sites known to project to the NTS including the PVH, lateral hypothalamus, central amygdala and dorsal raphe (Geerling and Loewy, 2006; Saper et al., 1976; Sawchenko and Swanson, 1982) (Figure S7B). As expected, PVH neurons labeled by NTS-injected beads are not neuroendocrine cells as evidenced by their lack of co-labeling following peripheral administration of the retrograde tracer, fluorogold, which is taken up by median eminence- and posterior pituitary-projecting neurons (Luther et al., 2002) (Figure S7C).

In agreement with previous results (Biag et al., 2012), retrogradely transported beads were found in the ventral zone of the medial parvicellular part of the PVH (PVHmpv) (Figure 7B). Notably, ChR2-mCherry-expressing ARC RIP-Cre fibers were found commingling with bead-positive neurons in the PVHmpv (Figure 7B). Light-evoked IPSCs were then assessed in bead^{+} or adjacent bead^{-} PVH neurons. Light-evoked IPSCs were observed in most (19 of 23) bead^{+} PVH neurons, i.e. neurons that project to the NTS (Figure 7C). The latency between onset of light and onset of IPSC was 3.4 ± 1.5 msec (mean ± SD, 19 neurons). In contrast, light failed to evoke IPSCs in nearly all (13 of 14) bead^{-} PVH neurons (Figure 7D). Thus, GABAergic ARC RIP-Cre neurons are selectively connected to NTS-projecting PVH neurons.

To test the specificity of NTS-projecting PVH neurons with respect to afferent input, we next determined if AgRP neurons, like RIP-Cre neurons, provide monosynaptic input. AgRP neurons are a useful comparator because, like RIP-Cre neurons, they release GABA, originate in the arcuate and project to the PVH, but in striking contrast with RIP-Cre neurons, AgRP neurons inhibit energy expenditure (Krashes et al., 2011) and, in addition, they also stimulate food intake (Aponte et al., 2011; Krashes et al., 2011). Connectivity between AgRP neurons and NTS-projecting PVH neurons was determined using similar methods to those described above except that *Agrp-ires-Cre* mice (Tong et al., 2008) were used to enable ChR2 expression (Figure 7E). Expressed ChR2 was functional as evidenced by light-evoked action potentials in AgRP neurons (Figure S7D). Consistent with previous reports (Cone, 2005), ChR2-mCherry-expressing AgRP fibers were found to heavily innervate the PVH, and to comingle with bead-positive neurons in the PVHmpv (Figure 7F). However, unlike the situation with RIP-Cre neuron ChR2-assisted circuit mapping, light-evoked IPSCs were absent in all (16 of 16) bead^{+} PVH neurons, i.e. neurons that project to the NTS (Figure 7G). In contrast, light evoked IPSCs were observed in 2 out of 9 bead^{-} PVH neurons (Figure 7H) with a latency between onset of light and IPSC in these two neurons of 3.5 and 5.7 msec. Afferent control of NTS-projecting PVH neurons by RIP-Cre but not AgRP neurons is consistent with the opposite and different functions of these two arcuate neurons, and demonstrates the specificity of the ARC RIP-Cre neuron → NTS-projecting PVH neuron connection.

The neural pathway by which NTS neurons regulate sympathetic outflow to brown adipose tissue has yet to be established. To address this, we tested for connections between the NTS and the raphe pallidus (RPa), a physiologically important hindbrain site where numerous

BAT sympathetic preautonomic neurons are located (Morrison and Nakamura, 2011). Retrograde beads were stereotaxically injected into the RPa of *Vgat-ires-Cre, lox-tdTomato* reporter mice (to allow for identification of GABAergic neurons (Vong et al., 2011)) (Figure 7I). Consistent with previous studies (Hermann et al., 1997; Yoshida et al., 2009), RPa-projecting neurons were found to be located in the MPO, DMH, PAG, DR and NTS (Figure S7E–G). Of note, 68 of the 143 RPa-projecting NTS neurons were GABAergic, as evidenced by colocalization of beads with tdTomato (Figure 7J). In contrast, few or no GABAergic RPa-projecting neurons were detected in other sites (MPO, DMH, PAG and DR) (Figure S7H). Thus, the NTS sends dense projections to the RPa and, notably, GABAergic input to the RPa comes predominantly from the NTS. ChR2-assisted circuit mapping was then used to confirm a GABAergic NTS → RPa synaptic connection. AAV-Flex-ChR2(H134R)-mCherry virus was injected into the NTS of *Vgat-ires-Cre* mice (Figure 7K) and the activity of ChR2 within NTS GABAergic neurons was functionally verified (Figure 7L). Light-evoked IPSCs were then assessed in randomly selected RPa neurons. Of note, light-evoked IPSCs were detected in 5 out of 8 RPa neurons (Figure 7M) with a latency between onset of light and IPSC of 3.1 ± 1.6 msec (mean ± SD, 5 neurons), and these were completely blocked by bicuculine (data not shown).

DISCUSSION

RIP-Cre neurons regulate energy balance (Chakravarthy et al., 2007; Choudhury et al., 2005; Covey et al., 2006; Kubota et al., 2004; Lin et al., 2004; Mori et al., 2009), however, as RIP-Cre neurons are located in many sites, the neurocircuit basis for this has been unknown. To address this, we undertook a multistep approach. By deleting VGAT and VGLUT2 from RIP-Cre neurons, we established that release of GABA, but not glutamate, from RIP-Cre neurons regulates energy balance. Remarkably, this regulation was specific for energy expenditure; food intake was entirely unaffected. Building on this, we hypothesized that GABAergic RIP-Cre neurons located specifically in the arcuate nucleus mediate this effect. Using a pharmacogenetic approach to test this, we selectively stimulated arcuate RIP-Cre neurons and found that this markedly increased energy expenditure; again, without any effect on food intake. Notably, pharmacogenetic stimulation of energy expenditure was entirely dependent upon release of GABA. These studies establish that synaptic release of GABA from arcuate RIP-Cre neurons selectively drives energy expenditure.

We then used ChR2-assisted circuit mapping to anatomically and functionally identify downstream neurons receiving synaptic GABAergic input from arcuate RIP-Cre neurons. We observed that arcuate RIP-Cre neurons project heavily and predominately to the paraventricular nucleus of the hypothalamus (PVH). This is notable since it has been proposed that GABAergic input to the PVH stimulates sympathetic outflow and brown adipose tissue (BAT)-mediated energy expenditure (Madden and Morrison, 2009). Importantly, PVH neurons, specifically those that project to the NTS in the brainstem, a site known to regulate energy expenditure (Cao et al., 2010), receive monosynaptic GABAergic input from arcuate RIP-Cre neurons. In summary, these studies have uncovered an arcuate nucleus-initiated neurocircuit that selectively drives energy expenditure.

Selective Regulation of Energy Expenditure

The ability of arcuate RIP-Cre neurons to regulate energy expenditure, without affecting food intake, is noteworthy. It is seen following genetic deletion of *Vgat* (Figures 2 and 3) and *Lepr* (Covey et al., 2006) in RIP-Cre neurons, and, importantly, also following acute pharmacogenetic stimulation of RIP-Cre neurons (Figure 5). The selectivity of arcuate RIP-Cre neurons for energy expenditure is remarkable since other arcuate neurons, for example AgRP and POMC neurons, coordinately regulate both food intake and energy expenditure.

This unique feature of arcuate RIP-Cre neurons is important because it provides a scheme for experimentally approaching forebrain control of energy expenditure. Specifically, neurons receiving GABAergic output from arcuate RIP-Cre neurons are likely to play important roles in regulating energy expenditure but not food intake. In the present study, as will be discussed below, we have used this approach to uncover an efferent circuit that likely drives energy expenditure (arcuate RIP-Cre GABAergic neurons → PVH neurons → NTS neurons).

Paraventricular Nucleus and Regulation of Energy Expenditure

Local application of $GABA_A$ receptor antagonist to the PVH decreases sympathetic outflow and BAT-mediated energy expenditure, suggesting that GABAergic input to the PVH drives energy expenditure (Madden and Morrison, 2009). The neurons providing this GABAergic input, however, have been unknown. The following five points strongly support the view that arcuate RIP-Cre neurons are a major source of this BAT-, energy expenditure-stimulating GABAergic input. First, *Rip-Cre*, $Vgat^{flox/flox}$ mice have reduced energy expenditure, altered BAT morphology, reduced BAT temperature and reduced *Ucp1* gene expression – all suggestive of low BAT activity (Figure 2). Second, *Rip-Cre*, $Vgat^{flox/flox}$ mice have reduced diet-induced thermogenesis (Figure 3). Third, *Rip-Cre*, $Vgat^{flox/flox}$ mice have an impaired catabolic and BAT thermogeneic response to leptin treatment (Figure 4). Fourth, GABA release by the arcuate subpopulation of RIP-Cre neurons stimulates BAT thermogenesis and energy expenditure (Figure 5). And fifth, arcuate RIP-Cre neurons project primarily and heavily to the PVH (Figure 6E, 7B).

We used ChR2-assisted circuit mapping to test the above-mentioned assertion, that RIP-Cre neurons provide important synaptic GABAergic input to PVH neurons. Connectivity, however, was observed for only a small subset (~15%) of randomly selected PVH neurons. This low rate of connectivity is related to complexity of the PVH, which contains numerous cell types each with unique function (Biag et al., 2012; Simmons and Swanson, 2009). These include a) neuroendocrine neurons that secrete either oxytocin, vasopressin, thyrotropin- or corticotropin-releasing hormone, b) non-neuroendocrine neurons that regulate feeding behavior via presently ill-defined pathways (Gold et al., 1977; Leibowitz, 1978), and finally c) non-neuroendocrine neurons that regulate either sympathetic or parasympathetic outflow (Geerling et al., 2010; Swanson and Sawchenko, 1983). As sympathetic outflow is the primary driver of brown adipose function and energy expenditure (Bachman et al., 2002; Bartness et al., 2010), the energy expenditure-promoting action of RIP-Cre neurons is likely mediated by a minor subset of non-neuroendocrine neurons, specifically, those that control sympathetic tone.

Role of NTS-Projecting PVH neurons

For reasons mentioned below, neurons in the NTS, and therefore the subset of PVH neurons projecting to the NTS, are strong candidates for mediating RIP-Cre neuron-driven energy expenditure. NTS neurons a) receive dense input from the PVH, b) are known to control sympathetic outflow (Andresen and Kunze, 1994; Guyenet, 2006), c) are labeled by the transneuronal retrograde tract tracer, pseudorabies virus, following its injection into brown adipose tissue (Bamshad et al., 1999; Cano et al., 2003; Oldfield et al., 2002), and d) have recently been shown to regulate brown adipose tissue function (Cao et al., 2010). To test if NTS-projecting PVH neurons are indeed a major target of GABAergic RIP-Cre neurons, we injected retrogradely transported florescent beads into the NTS (and, due to its close proximity, the nearby DMV) and performed ChR2-assisted circuit mapping. Of great interest, most NTS-projecting neurons receive synaptic GABAergic input from RIP-Cre neurons as assessed by light-evoked IPSCs in bead-positive PVH neurons (Figure 7C). In striking contrast, most other PVN neurons, i.e. those not projecting to the NTS, do not

receive GABAergic input from RIP-Cre neurons (Figure 7D). Thus, NTS-projecting PVH neurons are the major target of energy expenditure-regulating arcuate GABAergic RIP-Cre neurons.

AgRP neurons, unlike RIP-Cre neurons, are not synaptically connected to NTS-projecting PVH neurons (Figure 7G). This distinction is remarkable because, like RIP-Cre neurons, AgRP neurons are located in the arcuate, are GABAergic, and send very dense projections to the PVH. However, in sharp contrast with RIP-Cre neurons, AgRP neurons have qualitatively different functions - they inhibit, as opposed to stimulate, energy expenditure (Krashes et al., 2011; Tong et al., 2008), and, in addition, they also stimulate food intake (Aponte et al., 2011; Krashes et al., 2011). These different functions must be explained by differences in efferent circuitry. Consistent with this, the present study clearly demonstrates that such differences can robustly be resolved at the level of the PVH; RIP-Cre neurons are synaptically connected with NTS-projecting PVH neurons while AgRP neurons are not. These results suggest a means for deconvoluting complex circuitry that traverses the PVH. By using PVH-projecting neurons of defined function as the entry point, in this case AgRP versus RIP-Cre neurons, and by performing ChR2-assisted circuit mapping to identify PVH neurons which are synaptically downstream, in conjunction with retrograde tracers that subdivide PVH neurons based upon differential sites of projection, it is possible to ascribe function and to determine wiring diagrams of circuits that span three synaptically coupled sites.

Circuitry linking NTS neurons with BAT

The raphe pallidus (RPa) is a sympathetic preautonomic area which when activated potently stimulates BAT activity (Morrison and Nakamura, 2011). Indeed, the RPa → sympathetic preganglionic → postganglionic neuron → BAT circuit likely constitutes the final common pathway by which the brain controls BAT activity. With this in mind, our observation that most GABAergic input to RPa neurons comes from the NTS is of interest and suggests the following pathway: arcuate RIP-Cre GABAergic neurons → PVH neurons → NTS GABAergic neurons → RPa neurons → → → BAT activity. The inclusion of a second GABAergic neuron in this circuit, namely the NTS GABAergic neuron, allows for stimulation (disinhibition) of BAT activity by RIP-Cre GABAergic neurons. Future studies will be required to critically test the functionality, with respect to control of BAT activity, of the above-mentioned pathway. In total, the circuitry uncovered in this study provides a framework for understanding homeostatic regulation of BAT activity and energy expenditure.

EXPERIMENTAL PROCEDURES

Mice

All animal care and experimental procedures were approved by the Beth Israel Deaconess Medical Center Institutional Animal Care and Use Committee. *Rip-Cre* transgenic mice (Postic et al., 1999) were obtained from The Jackson Laboratory (#003573). *lox-Vgat* mice were generated previously (Tong et al., 2008). Chow (Teklad F6 Rodent Diet 8664) or high-fat, high-sucrose (Research Diets, D12331) diets were used.

Metabolic Studies

Food intake, body weight, fat mass, and locomotor activity was measured as described (Dhillon et al., 2006). Oxygen consumption was measured with indirect calorimetry (Columbus Instruments). iBAT temperature was measured as described (Enriori et al., 2011) with remote biotelemetry (IPTT-300, Bio Medic Data Systems).

Leptin Treatment Studies

Leptin's effects on body weight and food intake were measured as reported (Banno et al., 2010). Leptin's effects on iBAT temperature were assessed as reported (Enriori et al., 2011) in animals implanted with biotelemetry probes (as above). Leptin-induced STAT3 phosphorylation was assessed in *Rip-Cre, lox-GFP* mice using methods previously described (Vong et al., 2011).

Parmacogenetic Studies

AAV_8-Flex-hM3Dq-mCherry virus (Krashes et al., 2011) was stereotaxically injected into the arcuate of 5–6 wks old mice (for oxygen consumption and iBAT temperature studies) or 3–4 wks old *Rip-Cre, lox-GFP* mice (for electrophysiological studies). 2–3 wks following viral injection, electrophysiological responses of mCherry-expressing neurons to 5μM CNO or thermogenic responses of animals to 0.3 mg/kg CNO (i.p.) were tested. See also Extended Experimental Procedures.

ChR2-assisted Circuitry Mapping

AAV_8-Flex-ChR2(H134R)-mCherry virus was stereotaxically injected into sites of interest of 3–4 wks old mice (Atasoy et al., 2008; Zhang et al., 2007). 2–3 wks after viral injection, light-stimulated firing responses or IPSCs were tested by whole cell recordings. For retrograde beads-related studies, red or green beads (Lumafluor Inc.) were stereotaxically injected 5 days prior to electrophysiological studies. See also Extended Experimental Procedures.

Statistics

Statistics were performed with GraphPad Prism software.

Supplementary Material

Refer to Web version on PubMed Central for supplementary material.

Acknowledgments

The authors acknowledge J. Lu, J.B. Ding, and members of the Lowell lab for helpful discussion; Z. Yang, J. Yu, B. Choi, X. Hu, S. Ma, and D. Cusher for technical support; C.B. Saper for insightful suggestions and reading manuscript; K. Deisseroth for AAV-Flex-ChR2(H134R)-mCherry, and B.L. Roth for AAV-FLEX-hM3Dq-mCherry. This work was supported by grants: to BBL– R01s (DK089044, DK071051, DK075632), R37 DK053477, BNORC & BADERC Transgenic Core - P30DK046200 and P30DK057521; to DK – P&F from BADERC & BNORC - P30DK057521 and P30DK0460200; to QT –R01 DK092605, AHA SDG3280017; to PMF - NS0736313.

References

Alexander GM, Rogan SC, Abbas AI, Armbruster BN, Pei Y, Allen JA, Nonneman RJ, Hartmann J, Moy SS, Nicolelis MA, et al. Remote control of neuronal activity in transgenic mice expressing evolved G protein-coupled receptors. Neuron. 2009; 63:27–39. [PubMed: 19607790]

Andresen MC, Kunze DL. Nucleus tractus solitarius--gateway to neural circulatory control. Annu Rev Physiol. 1994; 56:93–116. [PubMed: 7912060]

Aponte Y, Atasoy D, Sternson SM. AGRP neurons are sufficient to orchestrate feeding behavior rapidly and without training. Nat Neurosci. 2011; 14:351–355. [PubMed: 21209617]

Atasoy D, Aponte Y, Su HH, Sternson SM. A FLEX switch targets Channelrhodopsin-2 to multiple cell types for imaging and long-range circuit mapping. J Neurosci. 2008; 28:7025–7030. [PubMed: 18614669]

Bachman ES, Dhillon H, Zhang CY, Cinti S, Bianco AC, Kobilka BK, Lowell BB. betaAR signaling required for diet-induced thermogenesis and obesity resistance. Science. 2002; 297:843–845. [PubMed: 12161655]

Bamshad M, Song CK, Bartness TJ. CNS origins of the sympathetic nervous system outflow to brown adipose tissue. Am J Physiol. 1999; 276:R1569–1578. [PubMed: 10362733]

Banno R, Zimmer D, De Jonghe BC, Atienza M, Rak K, Yang W, Bence KK. PTP1B and SHP2 in POMC neurons reciprocally regulate energy balance in mice. J Clin Invest. 2010; 120:720–734. [PubMed: 20160350]

Bartness TJ, Vaughan CH, Song CK. Sympathetic and sensory innervation of brown adipose tissue. Int J Obes (Lond). 2010; 34(Suppl 1):S36–42. [PubMed: 20935665]

Bass J, Takahashi JS. Circadian integration of metabolism and energetics. Science. 2010; 330:1349–1354. [PubMed: 21127246]

Biag J, Huang Y, Gou L, Hintiryan H, Askarinam A, Hahn JD, Toga AW, Dong HW. Cyto- and chemoarchitecture of the hypothalamic paraventricular nucleus in the C57BL/6J male mouse: A study of immunostaining and multiple fluorescent tract tracing. J Comp Neurol. 2012; 520:Spc1.

Cannon B, Nedergaard J. Brown adipose tissue: function and physiological significance. Physiol Rev. 2004; 84:277–359. [PubMed: 14715917]

Cano G, Passerin AM, Schiltz JC, Card JP, Morrison SF, Sved AF. Anatomical substrates for the central control of sympathetic outflow to interscapular adipose tissue during cold exposure. J Comp Neurol. 2003; 460:303–326. [PubMed: 12692852]

Cao WH, Madden CJ, Morrison SF. Inhibition of brown adipose tissue thermogenesis by neurons in the ventrolateral medulla and in the nucleus tractus solitarius. Am J Physiol Regul Integr Comp Physiol. 2010; 299:R277–290. [PubMed: 20410479]

Chakravarthy MV, Zhu Y, Lopez M, Yin L, Wozniak DF, Coleman T, Hu Z, Wolfgang M, Vidal-Puig A, Lane MD, et al. Brain fatty acid synthase activates PPARalpha to maintain energy homeostasis. J Clin Invest. 2007; 117:2539–2552. [PubMed: 17694178]

Choudhury AI, Heffron H, Smith MA, Al-Qassab H, Xu AW, Selman C, Simmgen M, Clements M, Claret M, Maccoll G, et al. The role of insulin receptor substrate 2 in hypothalamic and beta cell function. J Clin Invest. 2005; 115:940–950. [PubMed: 15841180]

Cone RD. Anatomy and regulation of the central melanocortin system. Nat Neurosci. 2005; 8:571–578. [PubMed: 15856065]

Covey SD, Wideman RD, McDonald C, Unniappan S, Huynh F, Asadi A, Speck M, Webber T, Chua SC, Kieffer TJ. The pancreatic beta cell is a key site for mediating the effects of leptin on glucose homeostasis. Cell Metab. 2006; 4:291–302. [PubMed: 17011502]

Cowley MA, Smart JL, Rubinstein M, Cerdan MG, Diano S, Horvath TL, Cone RD, Low MJ. Leptin activates anorexigenic POMC neurons through a neural network in the arcuate nucleus. Nature. 2001; 411:480–484. [PubMed: 11373681]

Dhillon H, Zigman JM, Ye C, Lee CE, McGovern RA, Tang V, Kenny CD, Christiansen LM, White RD, Edelstein EA, et al. Leptin directly activates SF1 neurons in the VMH, and this action by leptin is required for normal body-weight homeostasis. Neuron. 2006; 49:191–203. [PubMed: 16423694]

Enriori PJ, Sinnayah P, Simonds SE, Garcia Rudaz C, Cowley MA. Leptin action in the dorsomedial hypothalamus increases sympathetic tone to brown adipose tissue in spite of systemic leptin resistance. J Neurosci. 2011; 31:12189–12197. [PubMed: 21865462]

Fuller PM, Lu J, Saper CB. Differential rescue of light- and food-entrainable circadian rhythms. Science. 2008; 320:1074–1077. [PubMed: 18497298]

Geerling JC, Loewy AD. Aldosterone-sensitive neurons in the nucleus of the solitary tract: bidirectional connections with the central nucleus of the amygdala. J Comp Neurol. 2006; 497:646–657. [PubMed: 16739197]

Geerling JC, Shin JW, Chimenti PC, Loewy AD. Paraventricular hypothalamic nucleus: axonal projections to the brainstem. J Comp Neurol. 2010; 518:1460–1499. [PubMed: 20187136]

Gold RM, Jones AP, Sawchenko PE. Paraventricular area: critical focus of a longitudinal neurocircuitry mediating food intake. Physiol Behav. 1977; 18:1111–1119. [PubMed: 928534]

Guyenet PG. The sympathetic control of blood pressure. Nat Rev Neurosci. 2006; 7:335–346. [PubMed: 16760914]

Hermann DM, Luppi PH, Peyron C, Hinckel P, Jouvet M. Afferent projections to the rat nuclei raphe magnus, raphe pallidus and reticularis gigantocellularis pars alpha demonstrated by iontophoretic application of choleratoxin (subunit b). J Chem Neuroanat. 1997; 13:1–21. [PubMed: 9271192]

Krashes MJ, Koda S, Ye C, Rogan SC, Adams AC, Cusher DS, Maratos-Flier E, Roth BL, Lowell BB. Rapid, reversible activation of AgRP neurons drives feeding behavior in mice. J Clin Invest. 2011; 121:1424–1428. [PubMed: 21364278]

Kubota N, Terauchi Y, Tobe K, Yano W, Suzuki R, Ueki K, Takamoto I, Satoh H, Maki T, Kubota T, et al. Insulin receptor substrate 2 plays a crucial role in beta cells and the hypothalamus. J Clin Invest. 2004; 114:917–927. [PubMed: 15467830]

Lee JY, Ristow M, Lin X, White MF, Magnuson MA, Hennighausen L. RIP-Cre revisited, evidence for impairments of pancreatic beta-cell function. J Biol Chem. 2006; 281:2649–2653. [PubMed: 16326700]

Leibowitz SF. Paraventricular nucleus: a primary site mediating adrenergic stimulation of feeding and drinking. Pharmacol Biochem Behav. 1978; 8:163–175. [PubMed: 652826]

Lin X, Taguchi A, Park S, Kushner JA, Li F, Li Y, White MF. Dysregulation of insulin receptor substrate 2 in beta cells and brain causes obesity and diabetes. J Clin Invest. 2004; 114:908–916. [PubMed: 15467829]

Liu T, Kong D, Shah BP, Ye C, Koda S, Saunders A, Ding JB, Yang Z, Sabatini BL, Lowell BB. Fasting Activation of AgRP Neurons Requires NMDA Receptors and Involves Spinogenesis and Increased Excitatory Tone. Neuron. 2012; 73:511–522. [PubMed: 22325203]

Luther JA, Daftary SS, Boudaba C, Gould GC, Halmos KC, Tasker JG. Neurosecretory and non-neurosecretory parvocellular neurones of the hypothalamic paraventricular nucleus express distinct electrophysiological properties. J Neuroendocrinol. 2002; 14:929–932. [PubMed: 12472873]

Madden CJ, Morrison SF. Neurons in the paraventricular nucleus of the hypothalamus inhibit sympathetic outflow to brown adipose tissue. Am J Physiol Regul Integr Comp Physiol. 2009; 296:R831–843. [PubMed: 19129373]

Mori H, Inoki K, Munzberg H, Opland D, Faouzi M, Villanueva EC, Ikenoue T, Kwiatkowski D, MacDougald OA, Myers MG Jr, et al. Critical role for hypothalamic mTOR activity in energy balance. Cell Metab. 2009; 9:362–374. [PubMed: 19356717]

Morrison SF, Nakamura K. Central neural pathways for thermoregulation. Front Biosci. 2011; 16:74–104. [PubMed: 21196160]

Munzberg H, Flier JS, Bjorbaek C. Region-specific leptin resistance within the hypothalamus of diet-induced obese mice. Endocrinology. 2004; 145:4880–4889. [PubMed: 15271881]

Novak A, Guo C, Yang W, Nagy A, Lobe CG. Z/EG, a double reporter mouse line that expresses enhanced green fluorescent protein upon Cre-mediated excision. Genesis. 2000; 28:147–155. [PubMed: 11105057]

Oldfield BJ, Giles ME, Watson A, Anderson C, Colvill LM, McKinley MJ. The neurochemical characterisation of hypothalamic pathways projecting polysynaptically to brown adipose tissue in the rat. Neuroscience. 2002; 110:515–526. [PubMed: 11906790]

Petreanu L, Huber D, Sobczyk A, Svoboda K. Channelrhodopsin-2-assisted circuit mapping of long-range callosal projections. Nat Neurosci. 2007; 10:663–668. [PubMed: 17435752]

Pinto S, Roseberry AG, Liu H, Diano S, Shanabrough M, Cai X, Friedman JM, Horvath TL. Rapid rewiring of arcuate nucleus feeding circuits by leptin. Science. 2004; 304:110–115. [PubMed: 15064421]

Postic C, Shiota M, Niswender KD, Jetton TL, Chen Y, Moates JM, Shelton KD, Lindner J, Cherrington AD, Magnuson MA. Dual roles for glucokinase in glucose homeostasis as determined by liver and pancreatic beta cell-specific gene knock-outs using Cre recombinase. J Biol Chem. 1999; 274:305–315. [PubMed: 9867845]

Saper CB, Loewy AD, Swanson LW, Cowan WM. Direct hypothalamo-autonomic connections. Brain research. 1976; 117:305–312. [PubMed: 62600]

Sawchenko PE, Swanson LW. Immunohistochemical identification of neurons in the paraventricular nucleus of the hypothalamus that project to the medulla or to the spinal cord in the rat. J Comp Neurol. 1982; 205:260–272. [PubMed: 6122696]

Simmons DM, Swanson LW. Comparison of the spatial distribution of seven types of neuroendocrine neurons in the rat paraventricular nucleus: toward a global 3D model. J Comp Neurol. 2009; 516:423–441. [PubMed: 19655400]

Song J, Xu Y, Hu X, Choi B, Tong Q. Brain expression of Cre recombinase driven by pancreas-specific promoters. Genesis. 2010; 48:628–634. [PubMed: 20824628]

Spyer KM. Annual review prize lecture. Central nervous mechanisms contributing to cardiovascular control. J Physiol. 1994; 474:1–19. [PubMed: 8014887]

Swanson LW, Sawchenko PE. Hypothalamic integration: organization of the paraventricular and supraoptic nuclei. Annu Rev Neurosci. 1983; 6:269–324. [PubMed: 6132586]

Tong Q, Ye C, McCrimmon RJ, Dhillon H, Choi B, Kramer MD, Yu J, Yang Z, Christiansen LM, Lee CE, et al. Synaptic glutamate release by ventromedial hypothalamic neurons is part of the neurocircuitry that prevents hypoglycemia. Cell Metab. 2007; 5:383–393. [PubMed: 17488640]

Tong Q, Ye CP, Jones JE, Elmquist JK, Lowell BB. Synaptic release of GABA by AgRP neurons is required for normal regulation of energy balance. Nat Neurosci. 2008; 11:998–1000. [PubMed: 19160495]

van den Pol AN. Weighing the role of hypothalamic feeding neurotransmitters. Neuron. 2003; 40:1059–1061. [PubMed: 14687541]

Vong L, Ye C, Yang Z, Choi B, Chua S Jr, Lowell BB. Leptin Action on GABAergic Neurons Prevents Obesity and Reduces Inhibitory Tone to POMC Neurons. Neuron. 2011; 71:142–154. [PubMed: 21745644]

Wicksteed B, Brissova M, Yan W, Opland DM, Plank JL, Reinert RB, Dickson LM, Tamarina NA, Philipson LH, Shostak A, et al. Conditional gene targeting in mouse pancreatic ss-Cells: analysis of ectopic Cre transgene expression in the brain. Diabetes. 2010; 59:3090–3098. [PubMed: 20802254]

Wu Q, Boyle MP, Palmiter RD. Loss of GABAergic signaling by AgRP neurons to the parabrachial nucleus leads to starvation. Cell. 2009; 137:1225–1234. [PubMed: 19563755]

Yang Y, Atasoy D, Su HH, Sternson SM. Hunger states switch a flipflop memory circuit via a synaptic AMPK-dependent positive feedback loop. Cell. 2011; 146:992–1003. [PubMed: 21925320]

Yoshida K, Li X, Cano G, Lazarus M, Saper CB. Parallel preoptic pathways for thermoregulation. J Neurosci. 2009; 29:11954–11964. [PubMed: 19776281]

Zhang CY, Baffy G, Perret P, Krauss S, Peroni O, Grujic D, Hagen T, Vidal-Puig AJ, Boss O, Kim YB, et al. Uncoupling protein-2 negatively regulates insulin secretion and is a major link between obesity, beta cell dysfunction, and type 2 diabetes. Cell. 2001; 105:745–755. [PubMed: 11440717]

Zhang F, Wang LP, Brauner M, Liewald JF, Kay K, Watzke N, Wood PG, Bamberg E, Nagel G, Gottschalk A, et al. Multimodal fast optical interrogation of neural circuitry. Nature. 2007; 446:633–639. [PubMed: 17410168]

Research Highlights

1. Synaptic release of GABA but not glutamate from RIP-Cre neurons prevents obesity
2. RIP-Cre neurons in the arcuate stimulate energy expenditure by releasing GABA
3. RIP-Cre neurons mediate leptin action on energy expenditure but not on feeding
4. Arcuate RIP-Cre neurons directly inhibit NTS-projecting PVH neurons

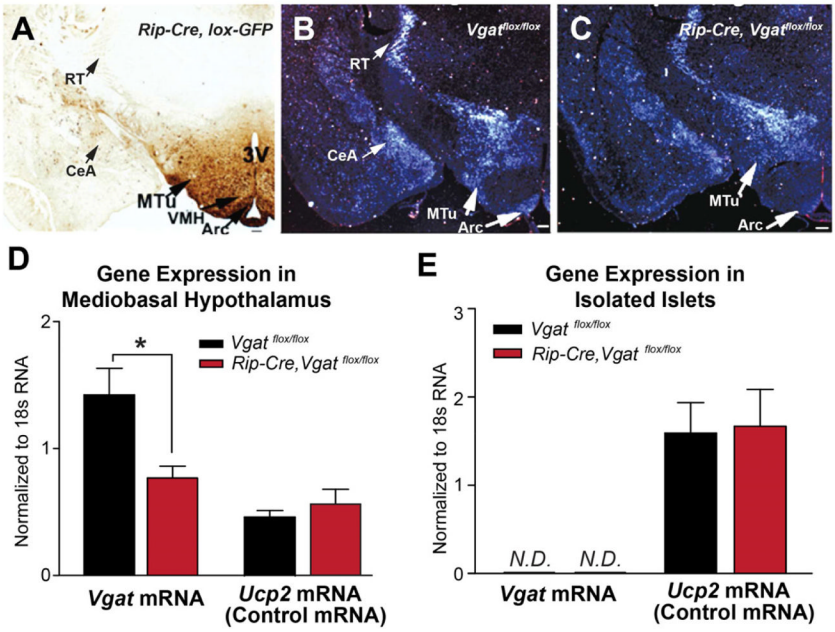

Figure 1. Generation of Mice Lacking VGAT in RIP-Cre Neurons

(A) Immunodetection of GFP in the brain of *Rip-Cre, lox-GFP* mice. 3V, third ventricle; VMH, ventromedial hypothalamus; MTu, medial tuberal nucleus; Arc, arcuate nucleus; RT, reticular nucleus of thalamus; CeA, central amygdala.

(B, C) *in situ* hybridization for *Vgat* mRNA in the brain of (B) control (*Vgat*$^{flox/flox}$) and (C) *Rip-Cre, Vgat*$^{flox/flox}$ littermates. Arrows indicate the regions with notable reduction of *Vgat* mRNA signal in *Rip-Cre, Vgat*$^{flox/flox}$ mice.

(D, E) Quantitative PCR results of *Vgat* mRNA in (D) mediobasal hypothalamus and (E) isolated pancreatic islets of 2-month old littermates (mean ± SEM; n=4). *N.D.*, non-detectable. *p< 0.05, unpaired t-tests.

See also Table S1.

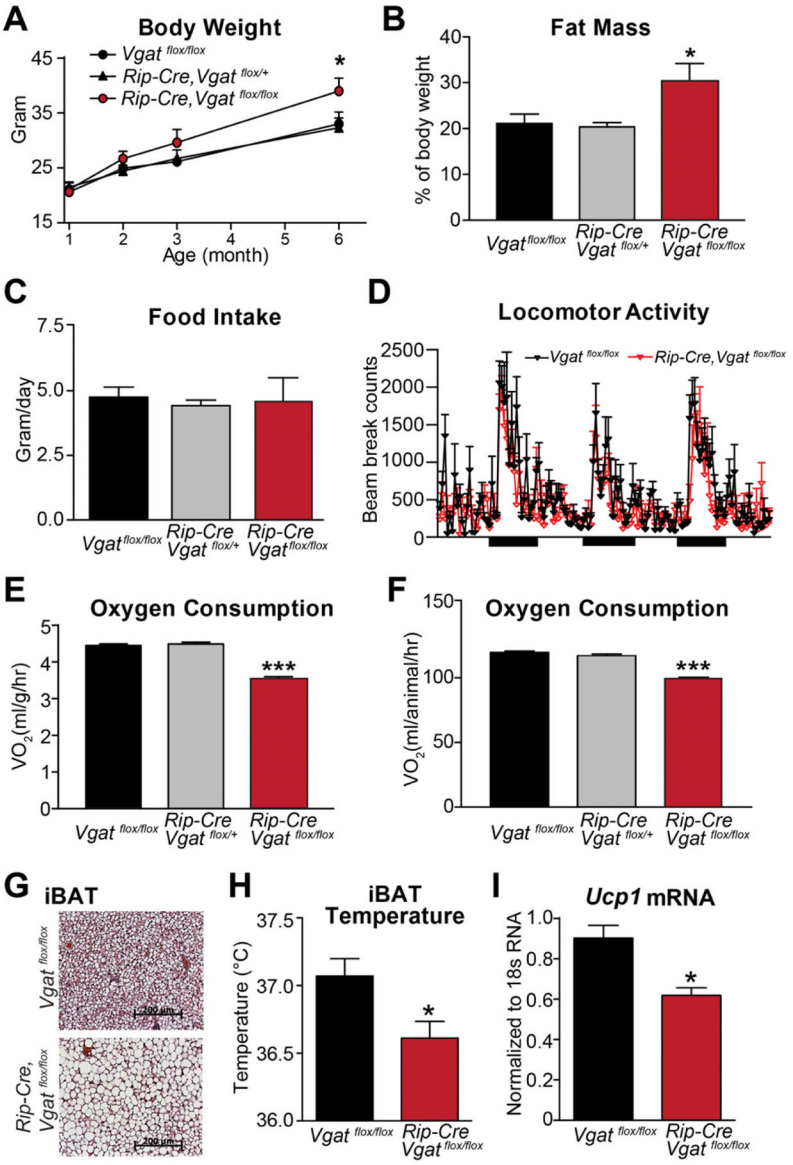

Figure 2. Energy Balance in Mice Lacking VGAT in Rip-Cre Neurons

(A) Body weight, (B) body fat mass (3-month old), (C) daily food intake (2-month old), and (D) locomotor activity (2-month old) of ad libitum chow-fed male littermates. (n=8–10). Black bars in (D) indicate dark cycles.

(E, F) Oxygen consumption of 2-month old male littermates expressed (E) per body weight and (F) per animal (n=8).

(G) H&E staining of brown adipose tissue from 2-month old littermates.

(H, I) (H) Temperature (n=12) and (I) *Ucp1* mRNA expression (n=4) in iBAT. Data are presented as mean ± SEM. *p< 0.05 and ***p<0.001, unpaired t-test compared with *Vgat*$^{flox/flox}$ group.

See also Figure S1 and S2.

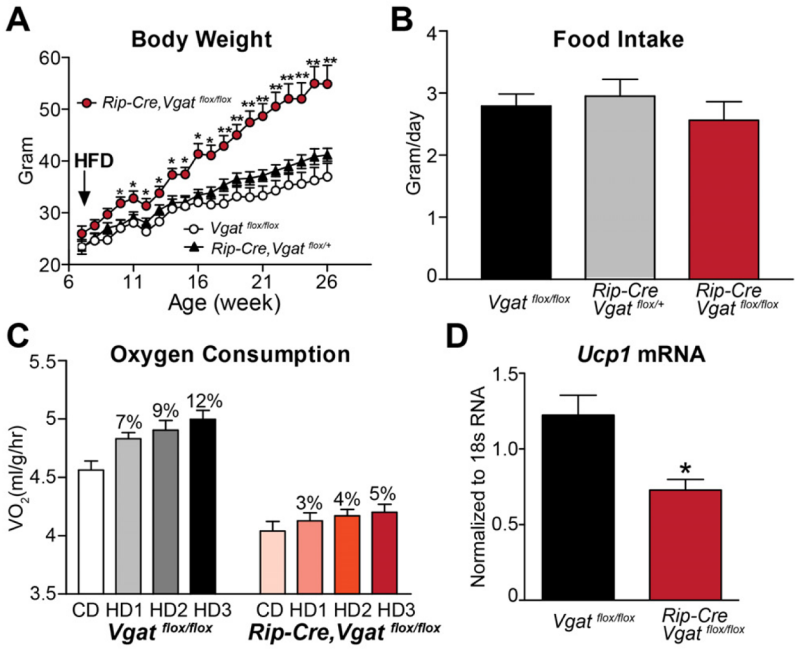

Figure 3. Diet-induced Obesity in Mice Lacking VGAT in RIP-Cre Neurons

(A) Body weight on HFD and (B) daily food intake averaged over the first two weeks on HFD (n=8–10).

(C) Oxygen consumption expressed per body weight during the transition from chow to HFD (n=8). CD = Averaged oxygen consumption over 3 days on chow. HD1, HD2 and HD3 = oxygen consumption during day 1, 2 and 3, respectively, on HFD. The percentage increase in oxygen consumption on HFD above that on chow diet is indicated above each bar.

(D) *Ucp1* mRNA level in iBAT of HFD-treated littermates (n=6–8).

Data are presented as mean ± SEM. *p< 0.05 and **p<0.01, unpaired t-test compared with $Vgat^{flox/flox}$ group.

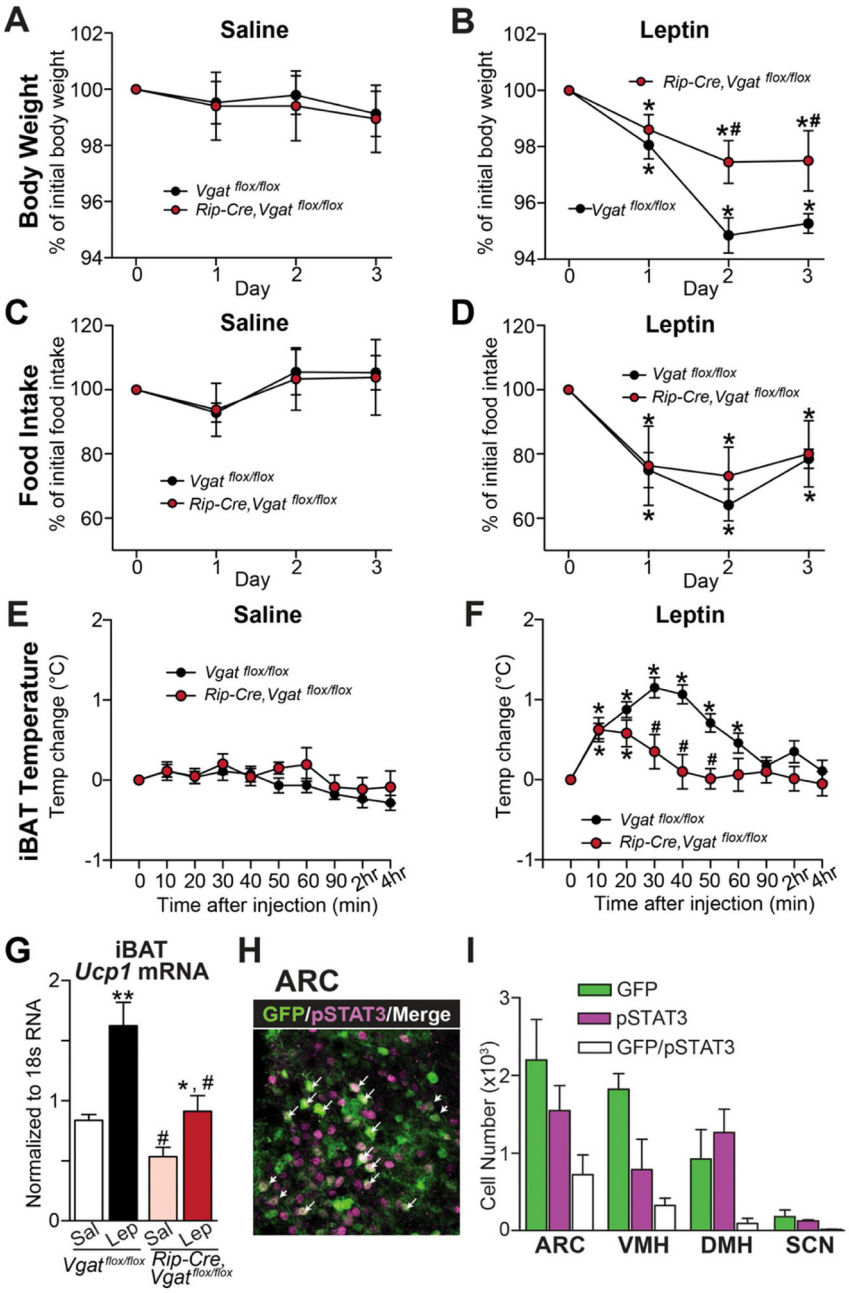

Figure 4. Response to Leptin in Mice Lacking VGAT in RIP-Cre Neurons

(A–F) The effects of saline or leptin on (A, B) body weight, (C, D) daily food intake, and (E, F) iBAT temperature in 2-month old male littermates (n=8–12). *p<0.05, paired t-test compared with animals of the same genotype before leptin injection (i.e. Timepoint 0); #p<0.05, unpaired t-test compared with control animals at given time point.

(G) *Ucp1* mRNA level in iBAT 4 hours after saline or leptin injection (n=6). *p<0.05 and **p<0.01, unpaired t-test compared with saline-injected animals of the same genotype; #p<0.05, unpaired t-test compared with $Vgat^{flox/flox}$ animals of the same treatment.

(H) Double immunohistochemistry for GFP (green) and leptin-induced phosphorylation of STAT3 (Tyr105, pSTAT3, magenta) in the ARC of *Rip-Cre*, *lox-GFP* mice. Arrows indicate the neurons with coexpression of GFP and pSTAT3.
(I) Quantification of the neurons that expressed GFP, pSTAT3, or both in the hypothalamic nuclei (n=3 mice).
Data are presented as mean ± SEM. See also Figure S3 and S5.

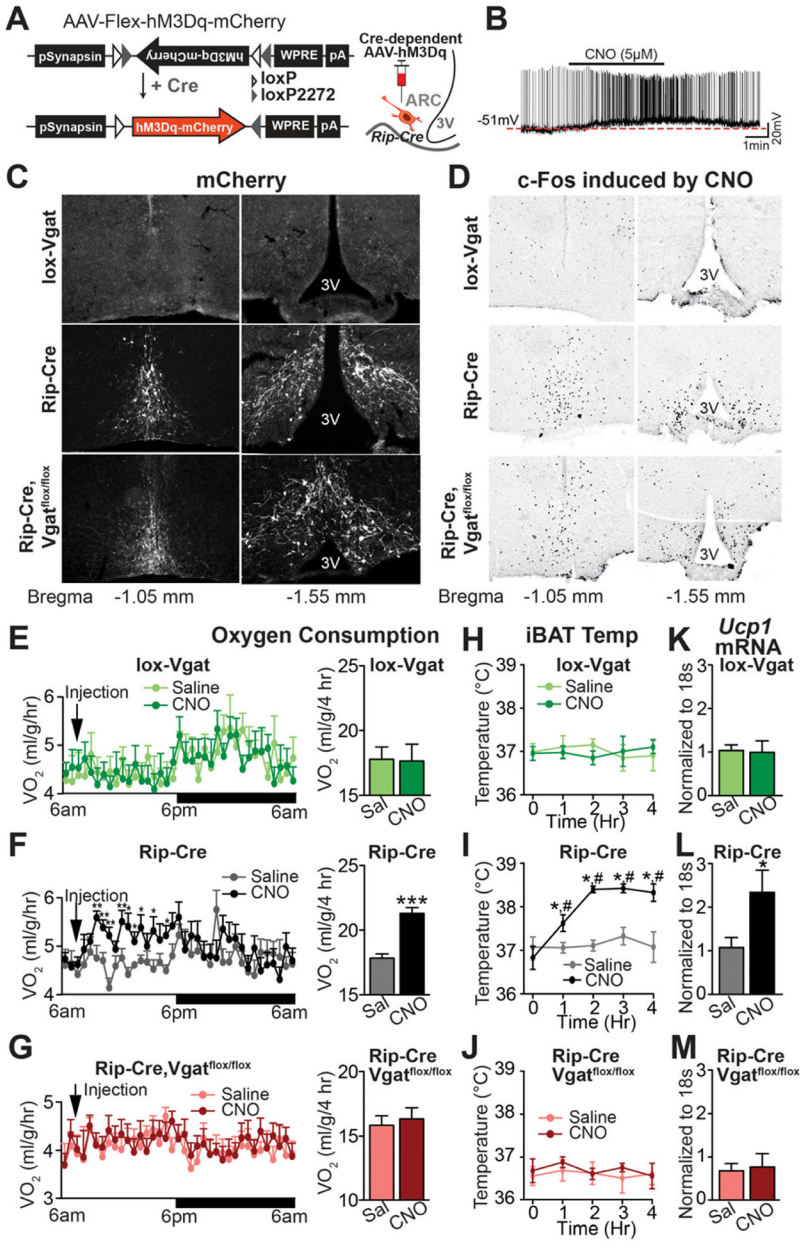

Figure 5. Pharmacogenetic Activation of ARC RIP-Cre Neurons

(A) Diagram of AAV-Flex-hM3Dq-mCherry (left) and schematic indication of the stereotaxic injection into the ARC of *Rip-Cre* transgenic mice (right).

(B) Representative whole cell, current-clamp recording from an ARC RIP-Cre neuron marked by mCherry fluorescence from a *Rip-Cre, lox-GFP* mouse injected with AAV-Flex-hM3Dq-mCherry virus.

(C, D) Immunohistochemistry for (C) mCherry and (D) CNO-induced c-fos (DAB, black stain) in the ARC of virus-injected $Vgat^{flox/flox}$ (top), *Rip-Cre* (middle), and *Rip-Cre,* $Vgat^{flox/flox}$ (bottom) male mice.

(E–G) Oxygen consumption over a 24-hour period (left panels) and during the first 4 hours (right panels) following i.p. injection of saline or CNO (n=8). *p<0.05, **p<0.01, ***p<0.001, paired t-tests compared to saline groups.

(H–J) iBAT temperature over 4 hours following saline or CNO injection (n=6–8). *p<0.01, paired t-test compared to animals of the same genotype before CNO injection; #p<0.01, paired t-test compared to saline-injected animals at given time point.
(K–M) *Ucp1* mRNA in iBAT 6 hours after saline or CNO injection (n=4–6). *p<0.05, unpaired t-test compared with saline-injected animals of the same genotype. Data are presented as mean ± SEM. See also Figure S4.

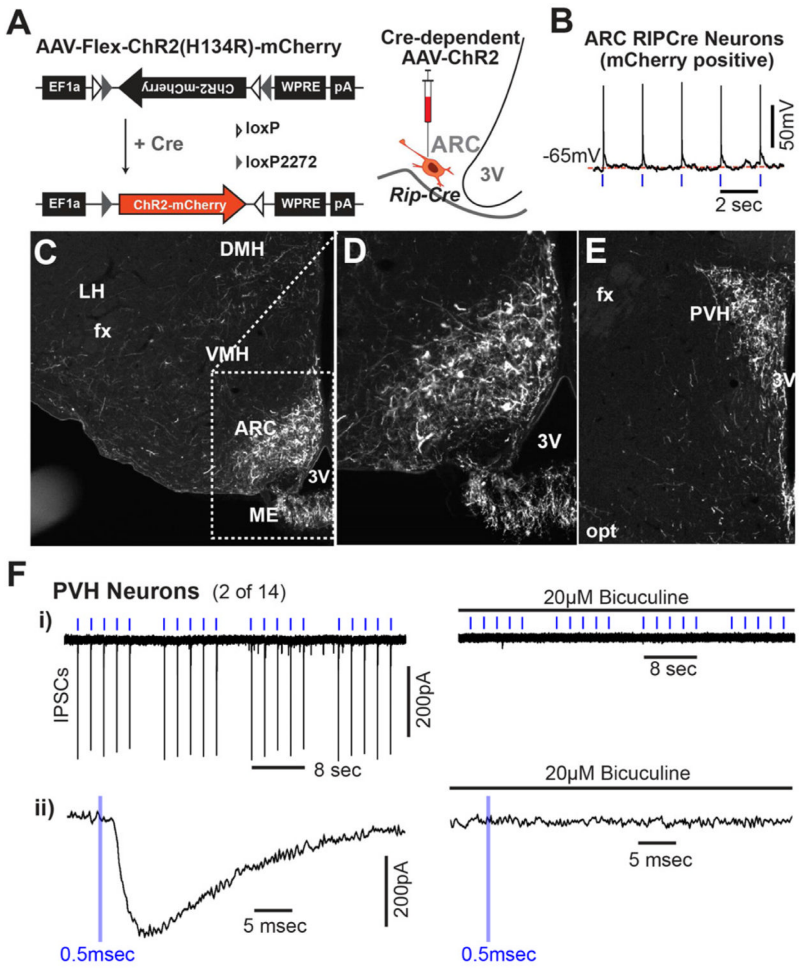

Figure 6. Projection of ARC RIP-Cre Neurons

(A) Diagram of AAV-Flex-ChR2(H134R)-mCherry (left) and schematic indication of the stereotaxic injection into the ARC of *Rip-Cre* transgenic mice (right).

(B) Representative voltage tracing showing light-driven spikes in a current-clamped arcuate neuron marked by mCherry fluorescence. Blue tickmarks represent 0.5msec light flashes at 0.5Hz.

(C–E) Immunohistochemistry for mCherry in the hypothalamus of virus-injected *Rip-Cre* transgenic mice. mCherry-expressing RIP-Cre neurons in the ARC are shown in (C) and in a zoomed view in (D). (E) mCherry-expressing RIP-Cre neuron fibers in the PVH. DMH: dorsomedial hypothalamus; VMH: ventromedial hypothalamus; ME: median eminence; ARC: arcuate nucleus; SCN: suprachiasmatic nucleus; PVH: paraventricular hypothalamus; 3V: third ventricle; fx: fornix; opt: optic tract.

(F) - i) Light-evoked IPSCs in a PVH neuron before (left) and after (right) the addition of 20μM bicuculine in response to clusters of light pulses. Blue tickmarks represent 0.5msec light flash at 0.5Hz. ii) Zoomed in view of response to a single pulse of light.

See also Figure S6.

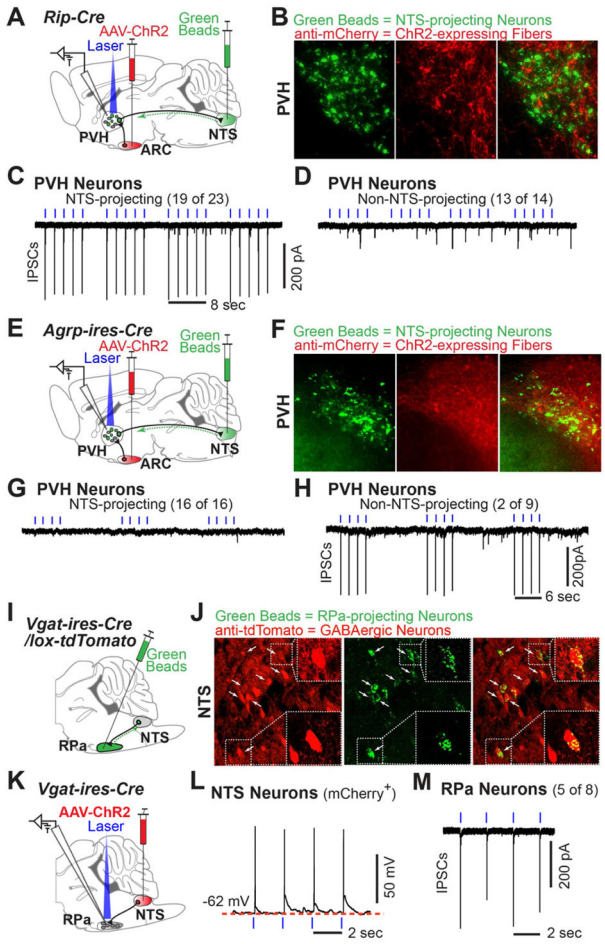

Figure 7. Downstream Neurocircuitry Engaged by ARC RIP-Cre Neurons

(A–D) (A) Diagram illustrating ChR2/retrobeads double-injection experiment in *Rip-Cre* transgenic mice. NTS: nucleus of the solitary tract. AAV-ChR2 = AAV-Flex-ChR2(H134R)-mCherry; Green Beads = fluorescent retrograde green beads. (B) Immunohistochemistry against mCherry (red) and native fluorescence of retrograde green beads (green) in the PVH. (C, D) Representative tracings of light-driven IPSCs recorded in (C) a PVH neuron with green beads (19 of 23), and in (D) an adjacent PVH neuron without green beads (13 of 14).

(E–H) (E) Diagram illustrating ChR2/retrobeads double-injection experiment in *Agrp-ires-Cre* mice. (F) Immunostaining against mCherry (red) and native fluorescence of retrograde green beads (green) in the PVH. (G, H) Representative tracings of light-driven IPSCs recorded in (G) a PVH neuron with green beads (16 of 16), and in (H) an adjacent PVH neuron without green beads (2 of 9).

(I–J) (I) Diagram illustrating retrograde tracing assay with green beads injected into the raphe pallidus (RPa) of *Vgat-ires-Cre, lox-tdTomato* mice. (J) Native fluorescence of green beads (green) and immunoreactivity of tdTomato (red) in the NTS. Arrows indicate the neurons labeled with both green beads (i.e. the neurons projecting to the RPa) and tdTomato (i.e. GABAergic neurons); two such neurons are zoomed in the dashed squares.

(K–M) (K) Diagram illustrating AAV-Flex-ChR2(H134R)-mCherry virus injected into the NTS of *Vgat-ires-Cre* mice. (L) Representative voltage tracing showing light-driven spikes in a current-clamped NTS neuron marked by mCherry fluorescence. (M) Representative

tracing of light-driven IPSCs recorded in RPa neurons (5 of 8). Blue tickmarks represent 0.5msec light flashes of 0.5Hz. See also Figure S7.